

# Ray Tracing Algorithm for Indoor Propagation

C.W. Trueman, R. Paknys, J. Zhao  
 EMC Laboratory  
 Concordia University  
 Montreal  
[Trueman@ece.concordia.ca](mailto:Trueman@ece.concordia.ca)  
[Paknys@ece.concordia.ca](mailto:Paknys@ece.concordia.ca)  
[Zhao@ece.concordia.ca](mailto:Zhao@ece.concordia.ca)

D. Davis  
 Dept. of Electrical Engineering  
 McGill University  
 Montreal  
[Don@ece.concordia.ca](mailto:Don@ece.concordia.ca)

B. Segal  
 Dept. of Otolaryngology  
 McGill University  
 Montreal  
[Segal@med.mcgill.ca](mailto:Segal@med.mcgill.ca)

*Abstract*-The fields due to a portable radio operated inside a hospital are of interest because of possible interference with hospital equipment. This paper presents an algorithm for finding ray paths from a handset to an observer using an “image tree” data structure. The algorithm finds all ray paths having field strength at the observer above a preset “threshold” value, no matter how many reflections are involved. The method is applied to compute the fields due to a handset in a small room, and the results are compared with measured field strengths.

## 1 Introduction

When a portable radio such as a cellular telephone is operated indoors, geometrical optics is often used to compute the handset’s fields[1]. If the observer is within sight of the handset, there is a “direct” path. There are often several paths involving one reflection: from the sidewalls of the room, from the floor, from the ceiling, from the wall behind the handset, or from the wall behind the observer. There are many paths having two reflections. Construction materials have sufficiently high permittivity that they are relatively good reflectors, hence a ray can undergo many reflections from the walls and floor before its field strength is reduced to an insignificant value. Hence some ray paths can include many reflections from the surfaces of the walls, floor and ceiling.

Ray paths are calculated by determining the location of an image source in each reflecting surface; multiple reflections use images of images. The conventional approach is to decide, a priori, to account for ray paths having  $N$  or fewer reflections, say  $N=3$  or 6 or 10, and to discard all other ray paths[1]. This paper presents a different approach to computing ray paths involving multiple reflections. We will decide, a priori, to include all ray paths that have field strengths larger than a “threshold” value. We then construct an “image tree”, with as many levels of images as needed to compute the field to the desired accuracy. Then for each observer, we use the pre-made image tree to compute actual ray paths from the handset to

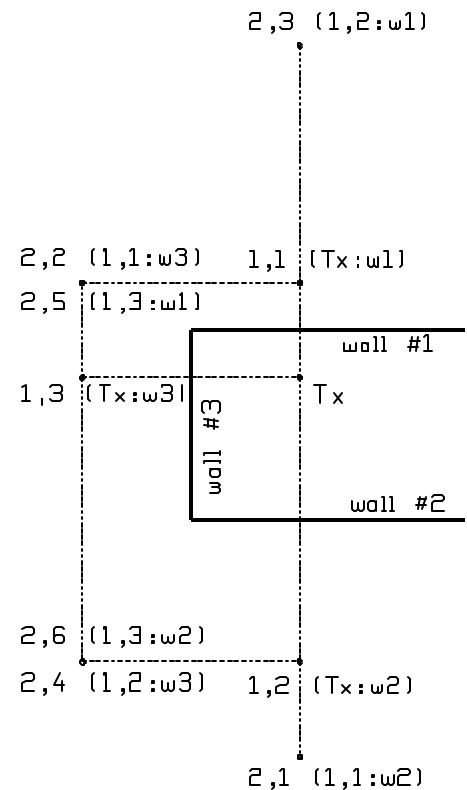


Figure 1 A system of three walls and a transmitter (Tx). The first two levels of images are shown.

that observer, and the field strength associated with each ray path.

The paper will conclude by comparing the computed field strength in a room with that obtained by direct measurement. Although there are many features of the actual room and the handset that cannot yet be included in the calculation, there is a reasonable correspondence between the measured and the computed field.

## 2 The Ray Tracing Algorithm

### 2.1 The Image Tree

Fig. 1 illustrates the construction of the set of images for a transmitter “Tx” and a system of three walls, leading to the tree structure of images shown in Fig. 2. The 1<sup>st</sup> level of the tree contains the image of the transmitter in each of the three walls, image sources (1,1), (1,2) and (1,3). Each image is uniquely identified by an ordered pair  $(i, j)$ . Images at level  $i$  in the tree are numbered sequentially,  $j=1,2,3$ . For our

system of three walls, these three image sources are sufficient to compute all ray paths having one reflection from the transmitter to the observer. The 2<sup>nd</sup> level of the tree contains the location of the image of each 1<sup>st</sup> level image source in each wall, except the wall that created the 1<sup>st</sup> level image. Thus for image source (1,1), which is an image in wall #1, there is image (2,1) in wall #2, and an image (2,2) in wall #3. Adding the images of sources (1,2) and (1,3) gives 6 images at the second level, as shown in Fig. 1. This is sufficient to compute all ray paths with one reflection or with two reflections from the transmitter to the observer. Note that the image tree is correct for *any* location of the observer, so the *same* image tree can be used to find the field for all possible observers.

The third level, the tree has the image of each 2<sup>nd</sup> level in two walls. Thus there are as many as twelve 3<sup>rd</sup> level images, and up to 24 images at the 4<sup>th</sup> level, and so forth. It may seem that the number of images will grow very rapidly. In fact this does not happen because the walls are not infinite planes. Consider image source S in Figure 3, which is an image in wall #S. At the next level, source S is imaged in wall #I to get image source I. Rays starting at I must lie in the solid angle between ray C and ray D in order that they pass through wall #I. These rays start at S and reflect from wall #I. But in turn rays starting at S must be reflections from wall #S. If points A and B are not within the physical area of wall #S, then we can discard image source #I. These geometrical considerations eliminate many image sources.

A stopping criterion is required, that indicates when no further images are needed. An obvious criterion is that if we try to create images at level  $N$ , but no images are created because no ray paths are

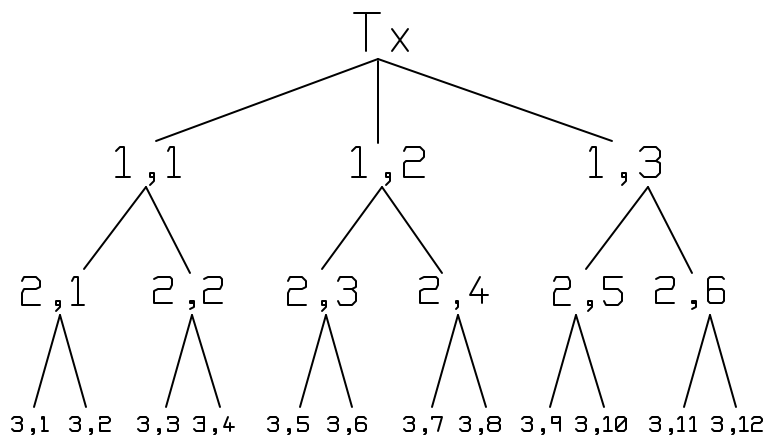


Figure 2 The image tree showing the transmitter and three levels of images.

possible, then we look no further for images. This is the case for a simple two wall system such as a corner reflector.

A more useful criterion is based on the observation in Fig. 1 that the images at level 2 are further from the walls than those at level 1. Similarly the images at level 3 are further from their associated walls than those at level 2. The largest possible field from an image is that evaluated at the nearest point on the surface of the wall giving rise to the image; since the field decreases as  $1/\text{distance}$ , as the images get further from the walls the maximum field goes down. Thus the user can specify a cutoff field strength for discarding images. When an image source is so far from its associated wall that the largest field falls below the cutoff, the image is discarded. The reflection coefficient is assumed to be unity during the construction of the image tree. Later, when the image location is used to find specific ray paths, the angle of incidence on each panel is known and then the reflection coefficient is fully accounted for.

On input the user specifies the radiated power  $P_r$  of the dipole antenna. The program computes the “isotropic level” field strength,

$$E_I = \sqrt{\frac{h_o P_r}{2\rho}}$$

where  $h_o$  is the intrinsic impedance of free space. This is the field strength that, radiated in one polarization uniformly over the radiation sphere, corresponds to a radiated power of  $P_r$  watts. The user specifies the “threshold” for discarding rays, in dB below the isotropic level. For example, to model a cellular telephone handset at 835 MHz with radiated power 600 mW, the isotropic level is 6 volts per meter at one meter from the antenna. If the user specifies a threshold of  $-65.56$  dB, then the cutoff field strength is 3.16 mV/m, and image sources which can never yield field strengths larger than 3.16 mV/m are discarded. A larger value for the threshold would include more rays in the computation but would increase the computation time. This is a very conservative criterion because it does not account for attenuation associated with the reflection coefficients of multiple reflections. Hence more image sources are included than may actually be needed.

Ref. [1] recognizes that the hierarchy of images is a tree data structure. But in Ref. [1], the number of reflections must be decided a priori and the tree is constructed only to a pre-set depth. In the present work, the user decides a priori the minimum field strength that should be considered, by choosing the threshold in dB below the isotropic field strength. The program itself decides to what depth the image tree should be built, depending upon the maximum field strength that each image source can give rise to. For example, in finding the fields in a 150 m corridor, if the source is at one

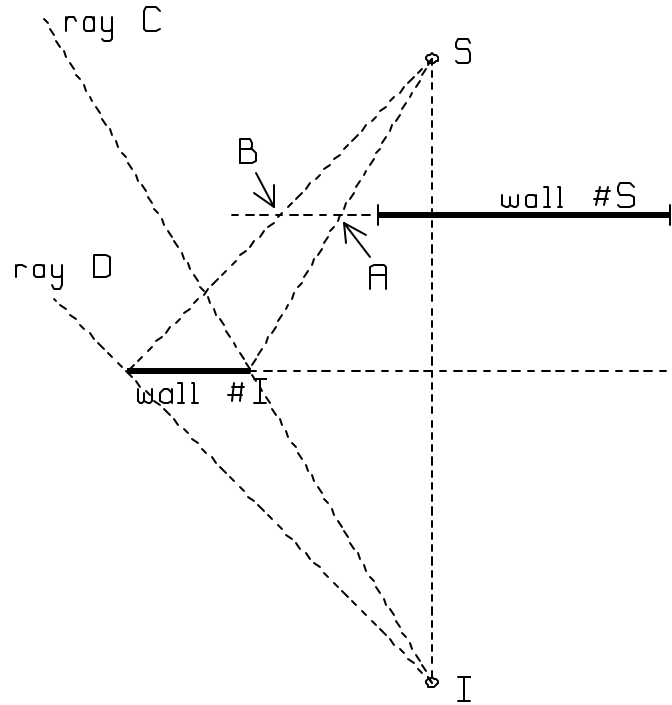


Figure 3 An image source S and its image I in wall #I

end and the receiver at the other, then many reflections from the walls can contribute to the receiver's field. Specifying the accuracy to which the field is needed is more meaningful in this case than simply deciding to include, say, up to 3 or 4 reflections in the computation.

## 2.2 Tracing Rays to an Observer

In a typical calculation, the field is required at many points along a line, or at many points covering a rectangular grid. Each such point is a "receiver". The image tree is constructed once, and then used to find the field at all of the receivers. Consider the image tree of Fig. 2, with three levels. To trace all possible rays with three reflections from the source to the observer, work through the tree as follows. First consider source (3,1). Trace a ray from (3,1) to (2,1), its parent in the image tree. The reflection point must lie within the physical area of the wall in which source (3,1) is an image, else discard the ray path. Then trace a ray from (2,1) to (1,1), the parent of (2,1). Again the reflection point must be physically within the area of the wall. Finally, trace a ray from (1,1) to the transmitter (Tx). If all three reflection points are real points, then calculate the field at the observer as follows. Start at the source and proceed to the reflection point associated with image (1,1). In a complex

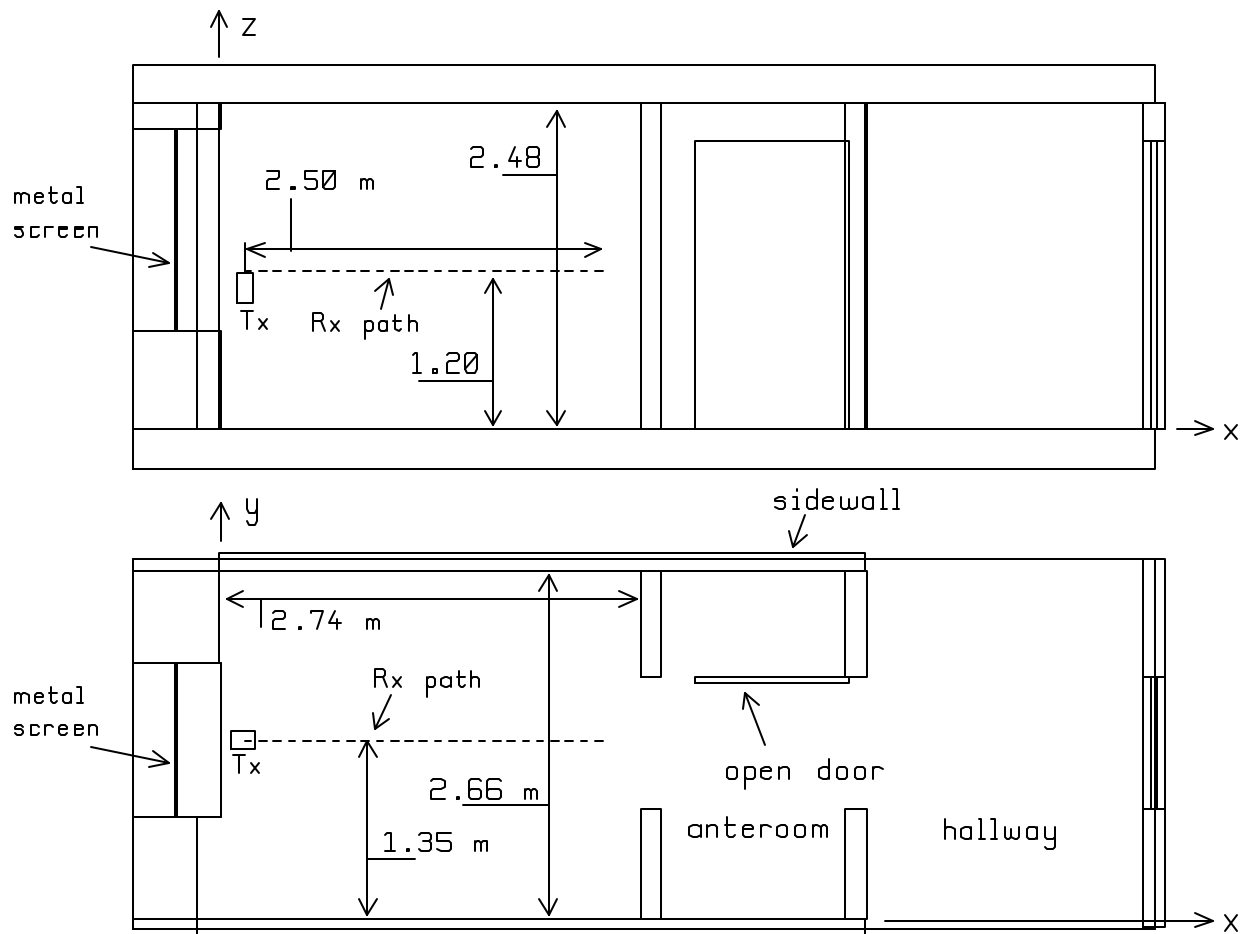


Fig. 4 The hospital clay-block room showing the location of the transmitter (Tx) and the measurement path for the receiver(dashed line).

problem, this ray may pass through one or more intervening walls; account for the transmission losses. Then account for the reflection coefficient associated with source (1,1) using the proper polarization and angle of incidence. Proceed to the reflection point for (2,1), then for (3,1). This gives us the field at the observer associated with one ray path, having three reflections.

Repeat the ray tracing outlined above for all the 3<sup>d</sup> level image sources, (3,2), (3,3), ..., to find all possible ray paths with three reflections. Then move up one level in the image tree. Start with image (2,1) and proceed up through the image tree to image (1,1) then to the transmitter (Tx), to identify one path having two reflections. This is done for all 2<sup>nd</sup> level images to find all the two-reflection paths. Then go to the 1<sup>st</sup> level, and find paths having one reflection for image sources (1,1), (1,2), etc. In this way all the possible ray paths from the transmitter to the receiver are found, including the associated field at the observer.

The search for ray paths using the image tree is repeated for each “receiver” that the user has specified.

### 2.3 Algorithm Application: A Hospital Clay Block Room

A comprehensive program of measurement of the field strengths in the hospital environment has been on-going for several years[2-7]. This paper evaluates the ray-tracing algorithm by comparing simulations with field measurements made in the small hospital room of clay block construction shown in Fig. 4. The transmitter is an analog cellular telephone handset, of an older design, operating at 835 MHz. The receiver is a dipole antenna mounted on a “robot”, which moves along the floor. The received signal is brought via a coaxial cable to a spectrum analyzer. The system records the field at preset intervals along the path, typically every 3.2 cm of distance traveled.

Fig. 4 shows the hospital room in which the measurement was made. At bottom, the plan view of the room shows that it is 2.74 m deep by 2.66 m wide by 2.48 m tall. The walls are clay block construction, 14 cm thick. The floor and ceiling are concrete with an embedded metal mesh. The lower half of the window at left has a metal screen outside the glass. There are walls and a doorway into a small anteroom, and then walls and a door to the hall. The door is modeled as open, made of wood and 4 cm thick. The wall on the opposite side of the hall, with its wooden door, is included in the computation.

The base of the antenna on the transmitter is located about 44 cm in front of the metal window screen, 1.2 m above the floor, and 1.35 m from the left-hand wall

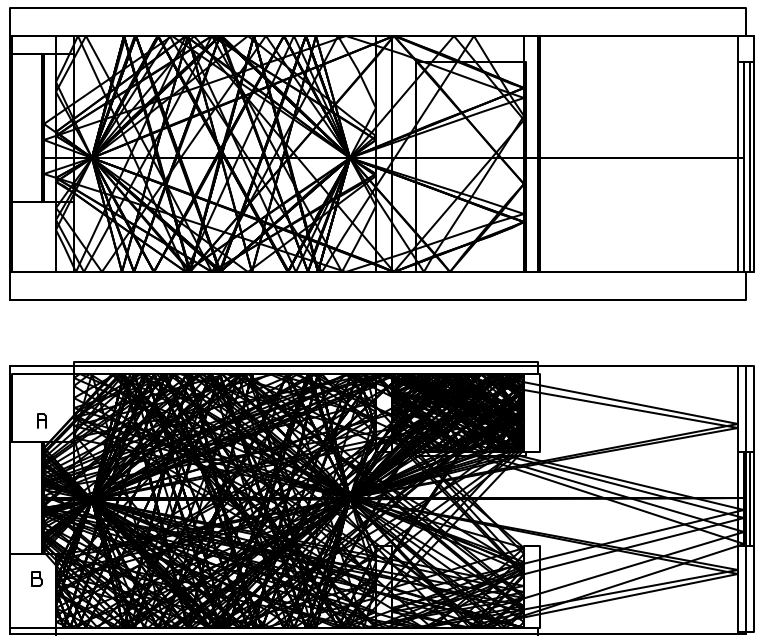


Figure 5 With the receiver positioned at the end of the 2.5 m path, the geometrical optics code computes the ray paths shown in this figure.

when the viewer is facing the window. The receiver dipole is moved by the robot along a path perpendicular to the window, displaced by 2 cm from the base of the antenna, hence 1.37 cm from the left-hand wall. The path runs from a point 44 cm from the window screen for a distance of 2.5 m.

### 2.3.1 Computing the Field

The geometrical optics code was run with a threshold of 65.56 dB. It creates 19 levels of images and 26,437 image sources for this problem, which has 17 wall panels including the floor and ceiling. Thus ray paths with up to 19 reflections are included in the calculation. Figure 5 shows all the ray paths used by the code, projected onto a horizontal plane in the plan view at bottom, and onto a vertical plane in the elevation at the top. Note that the surfaces of the walls near the window grille, at “A” and “B” in the figure, were not included as reflecting surfaces so some rays incorrectly pass through these surfaces. We note that many ray paths pass through the walls to the anteroom; this is correct and the transmission loss is accounted for. Rays become trapped in the rectangle formed by the sidewall, the door, the anteroom wall and the wall to the hall, and there are many, many rays bouncing around in this region before finding their way to the receiver. In the elevation view we see that there are many ray paths involving reflection from the floor and ceiling.

The handset in the measurement radiates 600 mW. An FDTD analysis of the handset shows that it radiates both an  $E_q$  and  $E_f$  component over the radiation sphere. With the handset oriented vertically, the azimuth radiation pattern in  $E_q$  is reasonably circular, with  $E_f$  having a figure-eight pattern about 17 dB down from  $E_q$ . The handset was represented in the geometrical optics analysis as an ideal dipole antenna that radiates 600 mW into  $E_q$ . It is intended in future work to incorporate the FDTD-computed handset fields over the radiation sphere into the geometrical optics analysis.

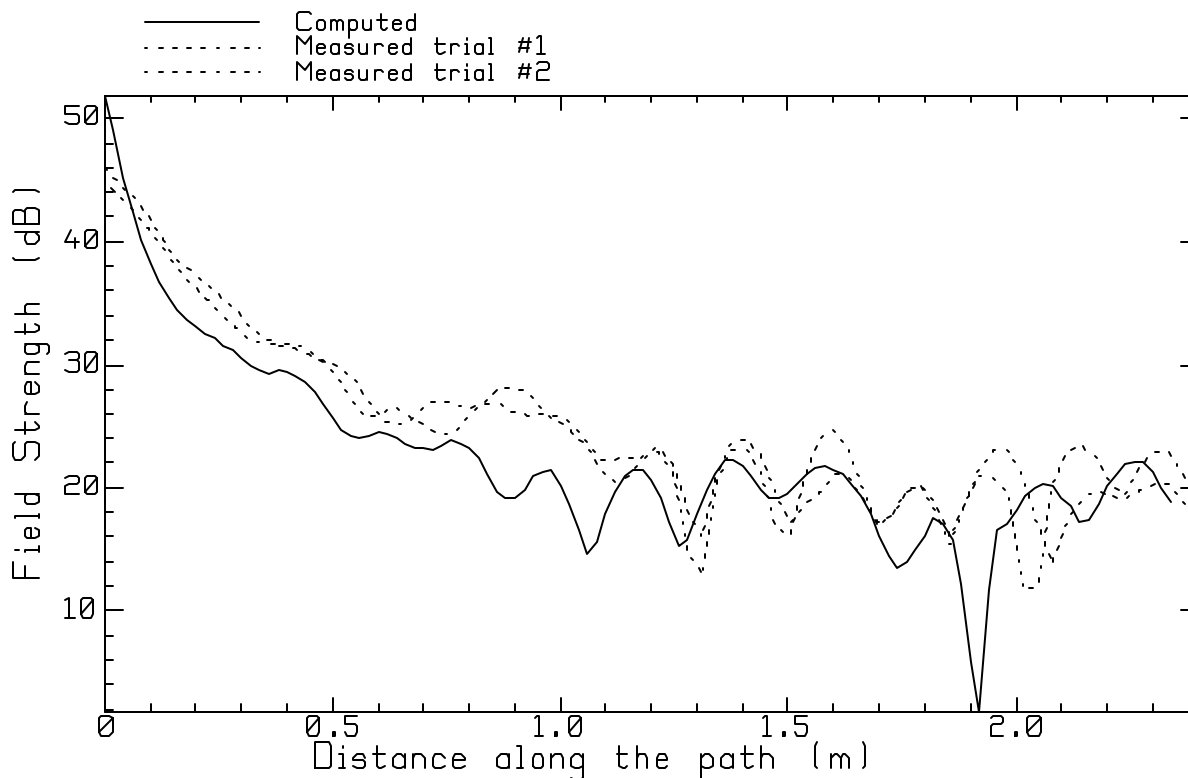


Fig. 6 Comparison of the computed and the measured field in the hospital room.

### 2.3.2 Computed vs. Measured Field Strength

Fig. 6 compares the computed and measured field strength along the path shown in Fig. 4, in dB above 1 volt/meter field strength. The dashed curves show two measurements done on the same day. The field strength close in to the transmitter is reasonably reproducible, to a distance of about 0.6 m. There are some differences near 0.5, 0.85 and 1.1 m. The minimum at 1.3 m differs between the two measurements. The peak at 1.35 m is reasonably consistent but that at 1.55 m differs between the two measurements. The peak at 1.8 m is almost identical. The measurements differ for distances greater than 1.9 m.

Both the measured field strength and the computed field strength correspond to 600 mW of radiated power. To a distance of about 0.8 m, the field associated with the direct ray dominates. The measured field is about 2 dB stronger than the computed field; but both decline with about the same slope. The field strength in this region is that of the transmitter plus the image of the transmitter in the metal screen covering the window. Moving the handset closer to or farther from the screen changes the phase relationship of the direct field and the field reflected from the screen, hence the net field strength.

Between about 0.8 m and 1.1 m distance, the measured field shows a maximum but the computed field has oscillations. From about 1.1 m to about 1.8 m distance the measurement and the computation both have oscillations and the locations of the maxima and the minima approximately correspond. In this region the peaks and minima are formed as the phase relationship changes between the direct ray from the transmitter, and the reflections from the two sidewalls in the room. Because of the transmitter's directional pattern in the vertical plane, the reflected ray from the floor and from the ceiling have only a minor influence on the vertical component of the field. At distances greater than about 1.8 m, the measurement and the computation correspond poorly, but the average field levels are very similar.

### 2.4 Conclusion

This paper uses geometrical optics to model indoor propagation. It presents a method for building a tree structure of image sources as the first step in computing the fields, and then using the same tree to find ray paths from the transmitter to each observation point. The user specifies a threshold to determine the weakest field to be accounted for, rather than the maximum number of reflections to be considered. The paper compares the computed field in a small room with measured data. It shows that the general behavior of the computed and measured fields is quite similar. Some features arising from the interference of the signal from the antenna with that from the room's sidewalls are reasonably well reproduced.

### References

1. M. Kimpe, H. Leib, O. Maquelin, and T. D. Szymanski, "Fast Computational Techniques for Indoor Radio Channel Estimation", *Computing in Science & Engineering*, pp. 31-41, Jan.-Feb., 1999.
2. P. Vlach, B. Segal and T. Pavlasek, "The Measured and Predicted Electromagnetic Environment at Urban Hospitals", *Proc. 1995 IEEE International Symposium on Electromagnetic Compatibility*, pp. 4-7, Aug. 14-18, 1995.
3. B. Segal, "Medical Equipment Malfunction: Risk and Minimization". In G.L. Carlo, editor, "Wireless Phones and Health: Scientific Progress", pp. 283-295, Kluwer Academic Publishers, Boston, Ma., 1998.

4. D. Davis, B. Skulic, B. Segal, P. Vlach and T. Pavlasek, "Variation of Emergency Room Electromagnetic Interference Potential", Proc. 1998 IEEE Antennas and Propagation Society International Symposium, pp. 1996-1999, Atlanta, Ga., June 21-25, 1998.
5. P. Vlach, B. Segal, J. LeBel and T. Pavlasek, "Cross-floor Signal Propagation Inside a Contemporary Ferro-concrete Building at 454, 862 and 1705 MHz", to be published in the IEEE Trans. On Antennas and Propagation.
6. D. Davis, B. Segal, T. Pavlasek, "Can Minimal-Separation Criteria Ensure Electromagnetic Compatibility in Hospitals?", AAMI Biomedical Instrumentation and Technology Journal, Vol. 33, No. 5, September/October 1999.
7. D. Davis, B. Segal, A. Cinquino, K. Hoege, R. Mastrocola and T. Pavlasek, "Electromagnetic Compatibility in Hospital Corridors", 1999 IEEE International Symposium on Electromagnetic Compatibility, pp. 268-272, Seattle, Wa., Aug. 2-6, 1999.